Development and characterization of novel agar and gelatin injectable hydrogel as filler for peripheral nerve guidance channels.

Tonda-Turo C, Gnavi S, Ruini F, Gambarotta G, Gioffredi E, Chiono V, Perroteau I, Ciardelli G.
Development and characterization of novel agar and gelatin injectable hydrogel as filler for peripheral nerve guidance channels.
JOURNAL OF TISSUE ENGINEERING AND REGENERATIVE MEDICINE (2014)
DOI: 10.1002/term.1902

Development and characterization of novel agar and gelatin injectable hydrogel as filler for peripheral nerve guidance channels

C. Tonda-Turo[1], S. Gnavi[2,3], F. Ruini[1], G. Gambarotta[2], E. Gioffredi[1], V. Chiono[1], I. Perroteau[2], and G. Ciardelli[1,4]

1 Department of Mechanical and Aerospace Engineering, Politecnico di Torino, Corso Duca degli Abruzzi 24, 10129 Torino, Italy

2 Department of Clinical and Biological Sciences, University of Turin, San Luigi Gonzaga Hospital, Regione Gonzole 10, 10043, Orbassano (Turin), Italy

3 Neuroscience Institute of the Cavalieri-Ottolenghi Foundation (NICO), University of Turin, Regione Gonzole 10, 10043, Orbassano, Turin, Italy

4 CNR-IPCF UOS, Via Moruzzi, 1, 56124 Pisa, Italy

Keywords: agar, gelatin, glial-like cells, hydrogel, injectable, peripheral nerve regeneration

Abstract

Injectable hydrogels are becoming increasingly interesting in the field of tissue engineering, thanks to their versatile properties and to the possibility to be injected into tissues or devices during surgery. In peripheral nerve tissue engineering, injectable hydrogels having shear-thinning properties are advantageous as filler of Nerve Guidance Channels (NGCs) to improve the regeneration process. In the present work, gelatin based hydrogels were developed and specifically designed for the insertion into the lumen of hollow NGCs through a syringe during surgery. Injectable hydrogels were obtained using an agar/gelatin 20/80 weight ratio, (wt./wt.) blend crosslinked by the addition of genipin (A/GL_GP). The physicochemical properties of the A/GL_GP hydrogels were analyzed, including their injectability, rheological, swelling and dissolution behaviour and their mechanical properties under compression. The developed hydrogel showed shear-thinning properties and was applied as filler of NGC.

The A/GL_GP hydrogel was tested *in vitro* using different cell lines among them Schwann cells have been used since they have an important role in peripheral nerve regeneration. Viability assays demonstrated the lack of cytotoxicity. *In vitro* experiments showed that the hydrogel is able to promote cell adhesion and proliferation. Two and three dimensional migration assays confirmed the capability of the cells to migrate both on the surface and within the internal framework of the hydrogel. These data show that A/GL_GP hydrogel has characteristics that make it a promising scaffold material for tissue engineering and nerve regeneration.

1. Introduction

Hydrogels are materials with wide application in the biomedical and pharmaceutical fields (Deligkaris et al. 2010, Slaughter et al, 2009), due to their structural and compositional similarities to the extracellular matrix (ECM). Many hydrogel types with different chemical and physical properties have been developed over the last decades using both synthetic water soluble polymers such as poly(acrylic acids), poly(acrylamides), poly(ethylene oxide), poly(vinyl alcohols), and poly(vinyl pyrrolidones) (Lyons et al., 2009; Mahoney et al., 2006; Marten et al., 2003) and natural polymers such as cellulose, hyaluronic acid, fibrin, chitosan, agar (Balgude et al., 2001; Crompton et al., 2007; Meena et al., 2007; Sakiyama et al., 1999). Hydrogels for biomedical applications can be properly designed to be injected through a syringe into the target tissue or device allowing minimally invasive surgical procedures. Among injectable hydrogels, shear-thinning hydrogels provide several advantages since they are pre-formed *ex vivo* and can be easily delivered by shear stress application during surgery (Guvendiren et al., 2012). Compared to standard hydrogels, which are liquid during injection and undergo a gelation process *in vivo*, the physico-chemical properties of shear-thinning hydrogels are not affected by the biological environment reducing the risk of liquid precursor leakage that can cause incomplete gel formation and toxicity. Moreover, shear-thinning hydrogels guarantee a rapid recovery of the elastic modulus after the shear stress is removed.

In peripheral nerve tissue engineering, hydrogels play a dual role, serving both as space filler to provide a substrate for axon regeneration and as carriers for bioactive molecule localized delivery. Filling the tubular nerve guidance channels (NGCs) sutured between the nerve stumps has been found to have a significant influence on axonal regeneration

across the gap (Wells et al., 1997; Willert et al., 2007). Compared to an empty tube or a tube containing physiological saline solution, faster axonal regeneration has been demonstrated when filling the tube with fibrin matrices (Williams et al., 1987), laminin containing gels (Madison et al, 1985), collagen (Cordeiro et al., 1989), hyaluronic acid (Chiono et al., 2009 - Seckel et al., 1995), and others. Among the various fillers used, shear-thinning hydrogels permitted to fill the tube during surgery through a preloaded syringe in a quick and safe way and reduced the risk of hydrogel leakage out of the tube. In the present work, hydrogel systems, based on agar (A) and gelatin (GL) crosslinked with genipin (A/GL_GP), were prepared and characterized to obtain injectable matrices that can be inserted into the NGC lumen during surgery. The final aim is to accelerate nerve regeneration and to reduce the risk of denervated muscle atrophy by enriching the nerve guides with hydrogels that can support Schwann cell adhesion and proliferation and neuritis outgrowth through the hydrogel.

GL is a commercially available biomaterial that is widely used in biomedical engineering for its biological properties due to its similarity, as adhesive protein, to the more expensive collagen. GP was used as GL crosslinking agent to increase its stability in water (Chiono et al., 2008; Tonda-Turo et al., 2011). Agars are cell-wall polysaccharides extracted with water from the Gelidiaceae and Gracilariaceae families of seaweeds and mainly composed of alternating (1-4)-D-galactose and (1-3)-3,6-anhydro-L-galactose repeating units (Freile-Pelegrın et al., 2005). Agar is soluble in water at temperatures above 65°C and it gels in a temperature range of 17-40°C. Agar forms shear-thinning hydrogels that can be easily inserted into a syringe and then injected into nerve guides during *in vivo* implantation (Quaglia, 2008; Steinert et al., 2008). The agar was added to GL solution with a weight ratio of 20/80 (wt./wt.) to

develop a gel with suitable injectability and providing biochemical cues for cell adhesion and proliferation.

The distinct ability of peripheral nerves to grow back to their targets it is due to the regenerative properties of its glia, the Schwann cells. Moreover, fibroblasts play a role in wound healing by secreting new extracellular matrix (ECM) and promoting tissue contraction resulting in scar formation. Additionally, they are thought to promote angiogenesis and inflammation by secreting proangiogenic and proinflammatory cytokines (Parrinello et al., 2010; Sorrell et al., 2009). Olfactory ensheathing cells (OEC) are specialized glial cells that guide the regeneration of non-myelinated olfactory axons from the peripheral nasal epithelium through the cribriform plate of the ethmoid bone into the olfactory bulb (OB). OEC represent an interesting candidate for cell therapy: several studies have demonstrated the great potential of OEC to promote axonal regeneration and functional recovery after CNS or PNS lesions (Guérout et al., 2011; Radtke et al., 2009).

In this work, the A/GL hydrogels crosslinked using GP (A/GL_GP) were characterized for their physico-chemical, rhelogical and mechanical properties, degradation kinetics and *in vitro* cellular adhesion, proliferation and migration. *In vitro* cell tests were performed using a mouse embryonic fibroblast cell line (NIH3T3), neonatal olfactory bulb ensheathing cells (NOBEC) and a Schwann cell line (RT4-D6P2T).

2. Materials and methods

2.1 Sample preparation

Agar (A, Sigma Aldrich) and gelatin (GL, type A from porcine skin, Sigma Aldrich) solutions at a concentration of 2% (wt./vol) were prepared in phosphate buffered saline (PBS). To prepare a solution of 10 ml, 0.04 g of A were dissolved in PBS at 90°C in an oven for one hour. Then, the A solution was kept under stirring at 50°C for 30 minutes and 0.16 g of GL were added. The resulting solution was kept under stirring at 50°C for 30 minutes and GP was added to the A/GL solution at a 2.5% wt./wt. amount with respect to the total amount of A and GL. The resulting solution (A/GL_GP solution) was kept under stirring at 50°C for 30 minutes and then the A/GL_GP solution was poured into Petri dish followed by 48 h air drying for flat membrane production (coded as "A/GL_GP films") and room temperature incubation for hydrogel gelification (coded as "A/GL_GP").

Uncrosslinked A/GL films and hydrogels were prepared as control following the same procedures described above except for GP addition. Moreover, uncrosslinked GL and A solutions (2% wt./vol.) in PBS were prepared as control at 90°C and 50°C, respectively.

A porous poly(caprolactone) (PCL; M_n: 80000 g/mol; Sigma Aldrich) tube was filled using the developed A/GL_GP hydrogel to assess the possibility to use the hydrogel as a NGC filler. A/GL_GP hydrogel was inserted into an insulin syringe before gelation and left overnight at room temperature to obtain gelation . Porous PCL guide having a diameter of 1.3 mm and a length of 15 mm were prepared as previously described by Tonda-Turo et. al (Tonda-Turo et al., 2011). Briefly, porous PCL guides were obtained by dip-coating of a rotating mandrel with PCL/poly(ethylene oxide) (PCL/PEO) blend solution followed by PEO solvent extraction. PCL/PEO 60/40 wt./wt. was selected as

the optimal composition to obtain porous membranes (PCL60i) with suitable morphological properties to ensure nutrient permeation and moderate stiffness.

After porous PCL tube fabrication, 20 µl of A/GL_GP hydrogel was then easily inserted into the hollow PCL guide through injection into the guide lumen by squeezing the pre-loaded syringe.

2.2 Sample characterization

2.2.1 Dissolution tests

The dissolution behaviour of A/GL_GP hydrogels was evaluated using a phosphate buffered saline (PBS) at pH 7.4 and each cylindrical sample (prepared in a 48-multiwell plate) was immersed into 5 ml of PBS. The dissolution degree was evaluated in PBS at 37°C after 1, 2, 4, 7, 14 days using A/GL_GP hydrogels dried in oven for 48 hours. The dissolution percentage was calculated as:

$$\Delta W_d(\%)=((W_0-W_d)/W_0)\cdot 100 \quad (1)$$

where W_0 and W_d are the hydrogel weights before and after dissolution. The solution pH was measured at the same time intervals of the dissolution test, to verify its stable value at around 7.4 (physiological pH). For each experimental condition, five samples were measured and the result was expressed as an average value ± standard deviation.

2.2.2 Fourier transform infrared-attenuated total reflectance spectroscopy (FTIR-ATR)

FTIR-ATR analysis of A, GL, A/GL and A/GL_GP films was performed in the 4000 cm^{-1}- 800 cm^{-1} wave number range using a Perkin Elmer Spectrum 100 equipped with an ATR attachment (UATR KRS5) with diamond crystal. Spectra were recorded with a resolution of 4 cm-1, a scan number of 16 and were analyzed by PerkinElmer Spectrum

Software. Five punctual measurements were performed on each sample and three samples for type were used.

2.2.3 Mechanical properties

Compressive stress–strain curves for the A, GL, A/GL and A/GL_GP hydrogels were obtained using a MTS QTest/10 device. Cylindrical specimens with 1 cm diameter and 1 cm thickness were used for the analysis. Samples were allowed to equilibrate for 24 hours at room temperature (20 °C) after sample preparation. The hydrogels were then placed in the centre of a flat compression stage and tested in triplicate at room temperature using a 10 N load cell. All the specimens were compressed at an uniform strain rate of 10 mm/min and the compressive force was applied along the height of the samples to have sample compression. Young's modulus (E, the slope of the linear elastic regime) was measured from the stress-strain curves. Three samples for type were used and the data were expressed as an average value ± standard deviation.

2.2.4 Rheological characterization and experimental injectability test

Rheological measurements were carried out on a strain-controlled rheometer (ARES, TA Instruments Inc., Waters LLC) with a torque transducer range of 0.2–2000 gf cm using a 25 mm parallel plates geometry. The general sample characterization was performed at 25°C through time (freq=1 rad/s and strain=0.5%), strain (freq=1 rad/s) and frequency (strain=0.5%) sweep tests. In particular, strain has been chosen in order to have a torque within the sensitivity of the instrument.

To demonstrate A/GL_GP injectability, hydrogels were inserted into a syringe (needle size 0,644 mm) and connected to a syringe pump (Aladdin-1000, World Precision

Instruments). A rate of 50 ml/hour was set and after 5 minutes the weight of the injected hydrogel was measured.

2.2.5 Fabrication and morphological characterization of A/GL_GP hydrogels filling PCL guide.

The A/GL_GP hydrogel was inserted into the tube lumen of a porous PCL hollow guide and frozen at -20°C overnight, then the frozen sample was subsequently freeze-dried at -20°C for 24 hours to obtain a dry hydrogel. The filled PCL tube was then fractured in liquid nitrogen and coated with silver using a sputter coater. The morphology of the section was investigated by scanning electron microscopy analysis (SEM) using a Philips 525M equipment at an accelerate voltage of 15 kV.

2.2.6 Cell culture and hydrogel sterilization

In vitro cell tests were performed using three different cell line: a mouse embryonic fibroblast cell line (NIH3T3), neonatal olfactory bulb ensheathing cells (NOBEC) and a Schwann cell line (RT4-D6P2T).

NOBEC cell line was kindly provided by Dr. Jacobberger (Comprehensive Cancer Center, Case Western Reserve University, 10900 Euclid Avenue, Cleveland, OH 4106-4944, USA). RT4-D6P2T and NIH3T3 cell lines were purchased from ATCC (American Type Culture Collection, 10801 University Blvd, Manassas, VA 20110-2209).

NIH3T3 cell line was originally established from primary mouse embryonic fibroblast cells that were cultured by the designated ATCC protocol. The NOBEC cell line was derived from primary cells dissociated from neonatal rat olfactory bulb and

immortalized by retroviral transduction of SV40 large T antigen (Goodman et al., 1993). NIH3T3, NOBEC and RT4-D6P2T were grown as described before (Tonda-Turo et al., 2013; Tonda-Turo et al., 2011). Before cell seeding, material samples were sterilized by 12 hours exposure to UV irradiation (UV lamp Technoscientific Co., wavelength 254nm) and then incubated overnight with complete DMEM (Dulbecco/s Modified Eagle Medium containing 10% Fetal Bovine Serum (Invitrogen)).

2.2.7 In Vitro Cell Tests on A/GL_GP hydrogels

2.2.7.1 Adhesion and proliferation assay

To assess the ability of A/GL_GP hydrogels to allow cell adhesion, three different cell lines were used. Adhesion and proliferation assays were performed as described before (Tonda-Turo et al., 2013; Tonda-Turo et al., 2011). NIH3T3, NOBEC and RT4-D6P2T cells were seeded in DMEM containing 10% FBS, at density of 2×10^3 cells cm^{-2} on both A/GL_GP hydrogel and control condition plates. After 3 hour (adhesion assay), 1, 3, 5, and 7 days in vitro (DIV) (proliferation assay), culture medium was removed, substrates with attached cells were rinsed with PBS with Ca^{2+} and Mg^{2+} and fixed by addition of 4% paraformaldehyde solution (PFA; Sigma-Aldrich). After 20 minutes, the PFA was removed and each plate was washed with PBS. Total nuclei were then stained for 30 minutes with Sytox Green (Sigma). Sytox Green is a nucleic acid stain and its absorption maximum is at 504 nm and its emission maximum is at 523 nm appearing green. Cells were photographed at Olympus IX50 microscope with a RS Photometrics camera. For each plate, four images were taken with a low magnification. The images were then acquired through the program Image Pro Plus and the number of adherent cells was counted with the program Image J. The experiment described above includes

the use of 3 sets of plates. Each set includes 3 hydrogels and 3 control plates. The counts obtained from assays were analysed, averaged, and expressed as percentage of adherent cells ± standard deviation.

To qualitatively evaluate cell adhesion and morphology, immunocytochemistry analysis was performed. Briefly, fixed cells were permeabilized with 0.1% Triton X-100 in 1X PBS for 5 minutes at room temperature and blocking solution (DAKO X0907 normal goat serum, diluted 1:10 in PBS) was applied for 1 hour at room temperature. F-actin was detected using FITC conjugated phalloidin (Sigma, diluted 1:1000 in blocking solution) by 1 hour incubation at room temperature following three wash steps of 5 minutes each. Vinculin was detected by overnight incubation with vinculin monoclonal antibody (Millipore, diluted 1:100 in PBS) followed by 1 hour incubation with goat-anti-mouse Alexa 488 secondary antibody (Invitrogen, diluted 1:400 in PBS). Fluorescnt images were acquired using a Nikon T-E microscope with a Plan Fluor 20× (Nikon) (numerical aperture (NA) = 0.45).

2.2.7.2 Adhesion assay: time lapse analysis

The three different cells were seeded at a cell density of 4×10^3 cells/cm^2 and allowed to adhere for 24 hours. Cells were kept at 37°C, 5% CO_2 in an incubator chamber for time-lapse video recording (Okolab). Cell movements were monitored with an inverted microscope (Eclipse Ti, Nikon) using Plan Fluor10×/0.25 NA or Plan Fluor 20×/0.45 NA Plan objectives (Nikon). Images were collected with CCD video cameras (Roper Scientific) at 30 min time intervals up to 48 hours, digitized and stored as image stacks using the MetaMorph 7.6.1.0 software (Universal Imaging Corp.). Image stacks were analyzed with the NIH image software (ImageJ).

2.2.7.3 Cell viability and cytotoxicity assay: 3-(4,5-dimethylthiazol-2-yl)-2,5-diphenyltetrazolium bromide (MTT) assay

3-(4,5-dimethylazol-2-yl)-2,5-diphenyltetrazolium bromide (MTT) assay was performed in order to evaluate A/GL-GP cytotoxicity as described before (Tonda-Turo et al., 2013). NIH3T3, NOBEC and RT4-D6P2T cell lines were seeded at a cell density of 2×10^3 cells/cm^2 on both A/GL_GP hydrogel and control condition plates. In order to quantify the cell number serial dilution was performed by plating 1×10^3, 2×10^3, 4×10^3, 8×10^3, 1.6×10^4, 3.2×10^4, and 6.4×10^4 per plate. After a 1, 3, 5 and 7 day incubation, 100 ul of MTT substrate (Sigma, 5 mg/ml in phosphate buffered saline) was diluted into 2 ml of complete medium and the cells were incubated at 37 °C for 4 h resulting in formazan formation. Then, the MTT solution was removed, and cells were washed twice with 1 ml of phosphate-buffered saline solution. Dimethylsulfoxide (DMSO; Sigma) was added to each well to dissolve the formazan. The plate was incubated at room temperature on a shaker for 30 min to enhance the dissolution of the formazan. A 100-µl aliquot from each well was transferred to a 96-well tissue culture plate.The spectrophotometric absorbance was measured at 570 nm wavelength, using DMSO as blank. Viability (%) was determined as (experimental group $A_{490\ nm}$/ control group $A_{490\ nm}$) × 100%. Each assay was performed in triplicate.

2.2.7.4 Apoptosis assay: dead cell stain

The three different cell line were seeded in complete medium at a density of 2×10^3 cells/cm^2 on polystyrene plates and hydrogels and were allowed to reach confluence. In control condition, apoptosis was induced by treating cells 24 hours with 100 µM cycloheximide (Sigma). Cycloheximide (CHX) is an antibiotic produced by *S. griseous*. Its main biological activity is translation inhibition in eukaryotes, resulting in cell

growth arrest and apoptosis induction. Apoptotic cells were stained with 166 μM Sytox green nucleic acid dye (Invitrogen) diluted in serum free medium (SFM) DMEM. SYTOX Green results in bright green fluorescence; it is excited at 488 nm, with an emission peak at 523 nm .

After 30 minutes, cells were rinsed with PBS with Ca^{2+} and Mg^{2+} and photographed using an Olympus IX50 microscope equipped with a RS Photometrics camera. For each plate, four images were taken with a low magnification. The images were then analysed through the program Image Pro Plus and the number of dead cells was counted with the program Image J. Experiments were performed as technical and biological triplicate for both control condition and hydrogel. The counts obtained from assays were analysed, averaged, and expressed as percentage of apoptotic cells/total cells ± standard deviation.

2.2.7.5 Three-dimensional migration assay: drop assay

Spheroid cell culture was performed using the drop method. NOBEC cells were detached from Petri dish using trypsin-EDTA, re-suspended in DMEM containing 10% fetal bovin serum (FBS) and centrifuged 4 minutes at 1000 round per minute (rpm). 2 x 10^5 NOBEC re-suspended in 20 μl containing 4 μl 2%FBS DMEM and 16 μl hydrogel solution were seeded in droplet into 3.5 cm polystyrene plates. After complete polymerization (15 minutes at room temperature), the hydrogel drops were overlaid with 2 ml 10% FBS DMEM and incubated in a humidified atmosphere of 5% CO_2 at 37°C. Medium was changed every two days, without disturbing the cell/hydrogel spheroid. NOBEC were stained using Cell Tracker Green (CTG, Invitrogen) following manufacturing's instructions. Fluorescence-images were recorded immediately (0 hr) and after 24, 48 and 72 hours intervals using Olympus IX50 microscope with a RS Photometrics camera. For each spheroid, four images were taken with a low

magnification to visualize spheroid expansion. Three separate experiments were run in technical triplicate. Spheroid perimeter was visualized in red (503 nm excitation filter), as a result of the red auto-fluorescence of GP. NOBEC were visualized in green (488 nm excitation filter). Cell motility was quantified by measuring the area occupied by the cells outside the spheroids perimeter by using ImageJ. Data were represented as mean ± standard deviation.

2.2.8 Statistics

The data were expressed as mean ± standard deviation, unless otherwise noted. Statistical analysis was carried out using single-factor analysis of variance (ANOVA). Values of * = $p<0.05$, ** = $p<0.01$,*** = $p<0.001$ were considered as statistically significant.

3. Results and discussion

3.1 Dissolution tests

The hydrogel dissolution was evaluated using dry samples. Figure 1 shows a high dissolution degree (15.9 ± 5,8 %) after 1 days and a dissolution of 41.3± 5.5 % after two weeks. The high dissolution in the first hours is fundamental to increase the hydrogel porosity allowing glial cells migration into the tube lumen and avoiding the risk of neuroma formation. Furthermore, the increased dissolution of the hydrogel with time is a required property to permit glial cells organization and Bünger bands formation.

3.2 Fourier transform infrared-attenuated total reflectance spectroscopy (FTIR-ATR)

In figure 2 reports FTIR-ATR exemplary spectra of A, GL, A/GL and A/GL_GP as derived from the analysis of 15 spectra for each sample type. The A spectrum (figure 2, curve A) showed the characteristic bands of agar (Praiboon et al., 2006) at 1370 cm^{-1}, 1070 cm^{-1}, 930 cm^{-1}, 890 cm^{-1} due to the ester sulfate, 3,6-anhydro-D-galactose, L-galactose-6-sulfate and C-H bending at the anomeric C of β-galactose residues, respectively. The FTIR-ATR spectra of the blends between A and GL (A/GL and A/GL_GP) showed the peaks of both GL and A. In figure 2, curves B, C and D spectra showed the characteristic bands associated with GL amide I (amide C=O stretching vibrations), amide II (amide N-H bending vibrations) and amide III (C–N stretching coupled with N–H in-plane bending vibrations), respectively at 1629 cm^{-1}, 1538 cm^{-1} and 1238 cm^{-1} (Muyonga et al., 2004). Moreover, no significant differences were detected between the A/GL and A/GL_GP spectra.

3.3 Mechanical properties

The Young modulus mean values and standard deviations for A, GL and A/GL_GP are reported in figure 3. The uncrosslinked A/GL hydrogels were very brittle and collapsed at low stress (< 2 kPa), for this reason they were not reported in the graph. At room temperature the E value of A (161.3 ± 31.1 kPa) was around 10 times higher than that of GL (18.9 ± 5.9 kPa). The E values for the A/GL_GP samples was 66.05 ± 7.78 kPa and was increased as compared to that of pure GL due to both the presence of 20 wt.% A and GP crosslinker.

3.4 Rheological characterization and experimental injectability test

Rheological measurements were carried out to analyze the A/GL_GP hydrogels viscoelastic behaviour at room temperature (25°C). The forces applied during sample loading probably induced a reorganization of the hydrogel structure and its relaxation was time-dependent (figure 4A). For this reason all the following rheological tests were performed after 1500 s. The dependence of elastic modulus (G') on the deformation amplitude was reported in figure 4B and the linear viscoelastic region was observed for strain values less than 0.7%. The elastic and the viscous (G'') moduli were plotted in figure 4C as a function of frequency. In the selected region, the material showed an elastic response, since moduli were independent on frequency and G' was higher than G''. This behaviour is typical of cross-linked materials (Macosko et al., 1994). Complex viscosity curve was also plotted for a general evaluation of hydrogel viscous properties. The slope of the regression line used for interpolating viscosity data was determined, providing information on the material non-Newtonian characteristics (Alzari et al., 2011). The viscosity decreased with increasing the frequency (figure 4D) indicating the plastic behaviour of the A/GL_GP hydrogel. Consequently, by increasing the shear rate, the A/GL_GP hydrogel can be easily injected.

Hydrogels were injected through a syringe (needle size G26) mounted in a volumetric syringe pump. A flow rate of 50 ml/hour allowed the deposition of 0.83 ml/min of hydrogel: after 3 minutes, the syringe pump was turned off and 2.5 g of delivered A/GL_GP hydrogel was weighted. After 30 seconds from injection, the Petri dish containing the hydrogel was inverted, without causing hydrogel flow, confirming the high viscosity of the hydrogel in the absence of shear stress (supplementary video/image S1).

3.5 Complete nerve guidance channel

Figure 5 shows an image of the SEM micrograph of a porous PCL hollow guide filled with the A/GL_GP hydrogel. The injected A/GL_GP hydrogel filled the inner cavity of the tube and was homogenously distributed. After freeze-drying, the hydrogel showed interconnected porosity and adhesion to the guide inner wall, indicating that the developed material and technology can be successfully implemented to engineer nerve guidance scaffolds with superior properties in term of nerve regeneration.

3.6 In vitro cell tests on A/GL_GP hydrogels

3.6.1 Cell adhesion assay

Cell adhesion is a key step for cell survival, growth and proliferation. Adhesion assay was carried out to evaluate the adhesion of NIH3T3, NOBEC and RT4-D6P2T cells on the surface of the A/GL-GP hydrogel. The blue colour of hydrogel after GP crosslinking induces autofluorescence (red) when observed under a fluorescence microscope.

The number of adherent cells was determined by counting stained nuclei and expressed as number of cells per mm^2 as reported in figure 6. Results showed that A/GL_GP hydrogel allowed cell adhesion, displaying the same adhesion rate of cells cultured in standard conditions on polystyrene plates (positive control), for all the three types (figure 6 A-C). The actin cytoskeleton is a highly dynamic network composed of actin polymers and a large variety of associated proteins. The function of actin cytoskeleton is to mediate a variety of essential biological functions, including intra and extracellular movement and structural support. Orientation distribution of actin filaments within a cell is, therefore, an important determinant of cellular shape, adhesion and motility. In order to have a better evaluation of cell adhesion, actin cytoskeleton and focal adhesion

complex were stained using FITC-conjugated phalloidin and anti-vinculin antibody respectively. NIH3T3, NOBEC and RT4-D6P2T cells seeded on A/GL-GP hydrogel showed a spread morphology similar to cells cultured in standard condition when stained with anti-S-100 antibody (representative pictures of RT4-D6P2T are reported in figure 6 panels D-E). Moreover, 5 hours after cell seeding, actin polymers were organized into a filament network (figure 6 panels H-I) even if focal adhesion junctions were not yet organized on both A/GL-GP hydrogel and control condition (figure 6 panels F-G).

Time lapse analysis was performed on NIH3T3, NOBEC and RT4-D6P2T seeded hydrogel in order to evaluate cell adhesion after 24 hours. These data provide qualitative information about cell adhesion, morphology and spreading on the biomaterial surface: 24 hours after seeding cells are still attached to the biomaterial and display a spread morphology. Moreover they could actively proliferate on the tested biomaterial (figure 7 and supplementary video S2-S3-S4).

3.6.2 Cell proliferation assay

The proliferation of NIH3T3, NOBEC and RT4-D6P2T cells cultured on A/GL_GP hydrogel was measured by quantifying the number of fluorescence labelled nuclei. Data analysis revealed a proliferation rate of cells plated on the A/GL_GP hydrogel comparable with that on polystyrene plates (positive control) (figure 8 A, B and C). The cell proliferation on both substrates increased with culture time; after 5 days, the cell monolayer was 70-80% confluent, after 7 days it was 80-100%. NIH3T3 displayed higher proliferation rate on both A/GL-GP hydrogel and control condition in comparison to both NOBEC and RT4-D6P2T. RT4-D6P2T displayed higher proliferation rate in comparison to NOBEC. The different proliferation rate is due to the

intrinsic characteristics of each cell line. Finally, after one day, cultured cells displayed a high actin cytoskeleton organization and focal adhesion complex formation, as shown by phalloidin and anti-vinculin immunostaining respectively (figure 8 L-S).

3.6.3 Cell viability and cytotoxicity assay: MTT assay

The colorimetric MTT assay was performed to evaluate the potential cytoxicity of the A/GL_GP hydrogel on the three different cell lines. A/GL_GP hydrogel did not exert any cytotoxic effect on cultured cells in comparison with standard control condition (figure 9), accordingly with results obtained in the cell proliferation assay. These data confirmed that A/GL_GP hydrogel is compatible with cell viability and proliferation.

3.6.4 Apoptosis assay: dead cell stain

To detect and quantify apoptosis of cells seeded on A/GL_GP hydrogel compared to control conditions, SYTOX Green labelling assay was performed as described in the method section. SYTOX Green nucleic acid stain is a green-fluorescent nuclear and chromosome counterstain that does not cross live cell intact membranes, whereas it penetrates dead cell compromised membranes. NIH3T3, NOBEC and RT4-D6P2T cells were cultured on polystyrene plates (positive control) and A/GL_GP hydrogel. Few apoptotic nuclei were observed in cells plated on A/GL_GP hydrogel or on control, confirming the good viability of the cells cultured on the hydrogel. The counts obtained from assays were analyzed and expressed as a percentage of apoptotic nuclei/total nuclei ± standard deviation. The percentage of apoptotic cells cultured on control condition and on A/GL-GP hydrogel were 0.14 ± 0.01%, 0.16 ± 0.02% for NIH3T3; 0.20 ± 0.02%, 0.22 ± 0.02% for NOBEC and 0.15 ± 0.03%, 0.11 ± 0.05% for RT4-D6P2T respectively. The percentage of apoptotic cells following cycloheximide treatment increased to 98.6 ± 1.02%, 96.4 ± 2.02% and 97.5 ± 1.14% for NIH3T3,

NOBEC and RT4-D6P2T respectively. Therefore, no statistically significant differences between the percentage of apoptotic cells detected on control condition and on A/GL-GP hydrogel were observed, confirming cell viability on the prepared biomaterial.

3.6.5 Three-dimensional migration assay: drop assay

In nerve tissue engineering, cell migration is a fundamental requirement for the design of internal fillers for bioengineered guides, allowing Schwann cell spreading and neuritis outgrowth through the graft. Cell migration through extracellular matrices is a key step in peripheral nerve regeneration. In fact, highly viscous hydrogels may obstruct the path for axonal growth toward the distal stump impeding the complete regeneration. *In vitro* migration assay was performed in order to test the capability of the biomaterial to allow cell migration due to its porous structure. Figure 10 shows that the number of NOBEC migrating outside a drop of A/GL_GP hydrogel increased with time, confirming the cell ability to migrate through the hydrogel. This migration is evidently facilitated by the A/GL_GP hydrogel porous structure.

4. Conclusion

An hydrogel based on A/GL_GP blend was prepared showing suitable rheological properties for its application as NGC filler by syringe injection. Biological characterisation showed that fibroblasts, olfactory bulb ensheathing cells and Schwann cells in contact with the hydrogel had normal cell morphology, viability and proliferation patterns, similar to those of the positive control. The porous structure of the hydrogel allowed cell migration both in two-dimensional and three-dimensional migration assay. A/GL_GP hydrogel supported cell adhesion, proliferation and migration which are required properties for a filler material in peripheral nerve

regeneration. Future works will be addressed to load specific biomolecules (such as growth factors) into the hydrogel filler. The mild conditions for hydrogel preparation (low temperature and physiological pH) can be advantageous for the incorporation of bioactive molecules avoiding their denaturation, while hydrogel microporosity can allow sustained biomolecule delivery over days to weeks period.

Acknowledgments

This work was supported by the Regione Piemonte ("Bando Ricerca Sanitaria Finalizzata") and the Compagnia di San Paolo ("MOVAG"). A special thanks to Tullio Genova, Daniele Avanzato (Department of Life Sciences and Systems Biology, Torino) and to Anabella Mancardi (Neuroscience Institute of the Cavalieri-Ottolenghi Foundation) for time lapse analysis and to Silvia Grifoni for graphical support.

FIGURE

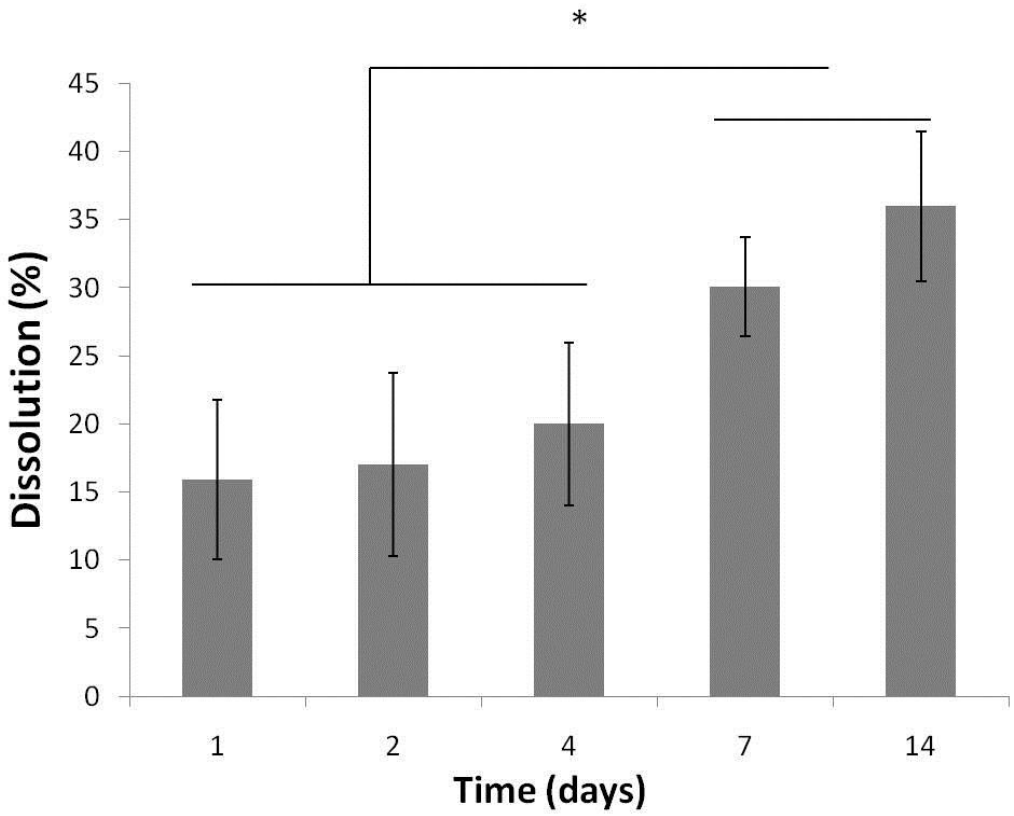

Figure 1. Dissolution degree. The dissolution degree evaluated after 1, 2, 4, 7, 14 days on dried A/GL_GP.

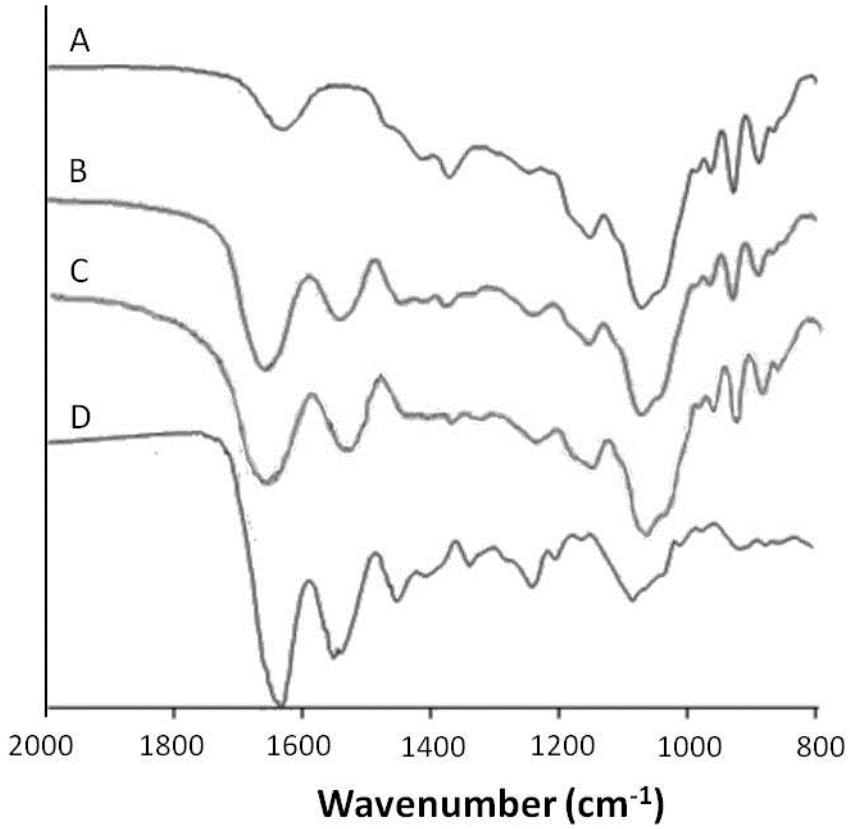

Figure 2. FTIR_ATR analysis. FTIR-ATR spectra of (A) A, (B) A/GL, (C) A/GL_GP, (D) GL.

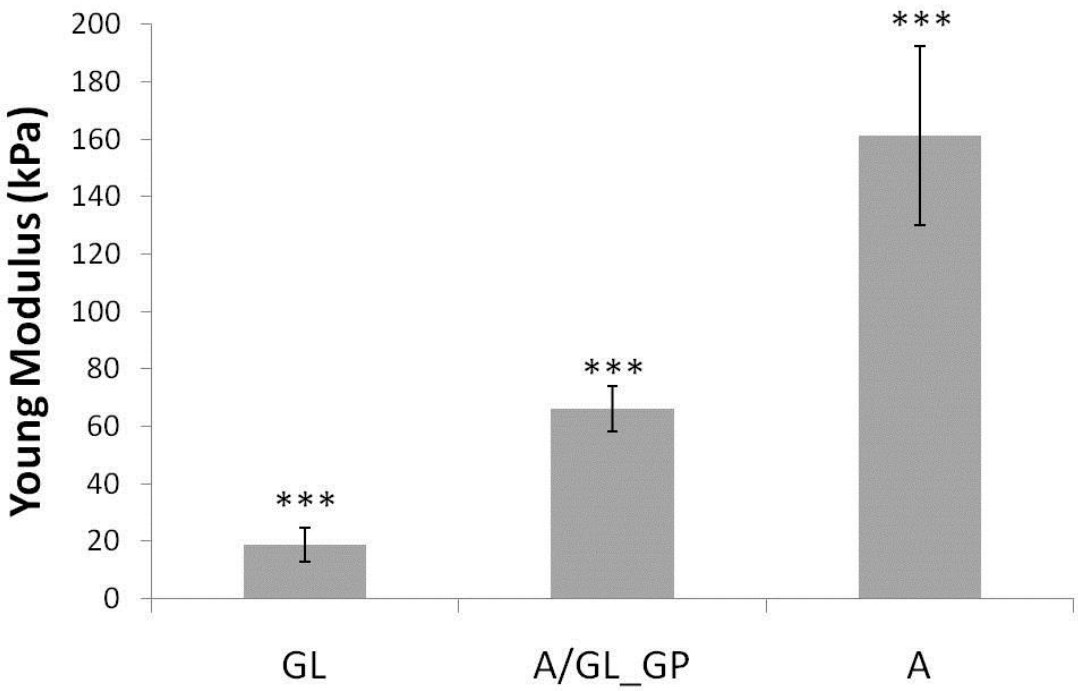

Figure 3. Mechanical characterisation. Young modulus histograms for A, GL and A/GL_GP. A significant difference was observed between the three samples (ANOVA one-way, post hoc Bonferroni, * = $p \leq 0.05$; ** = $p \leq 0.01$; *** = $p \leq 0.001$).

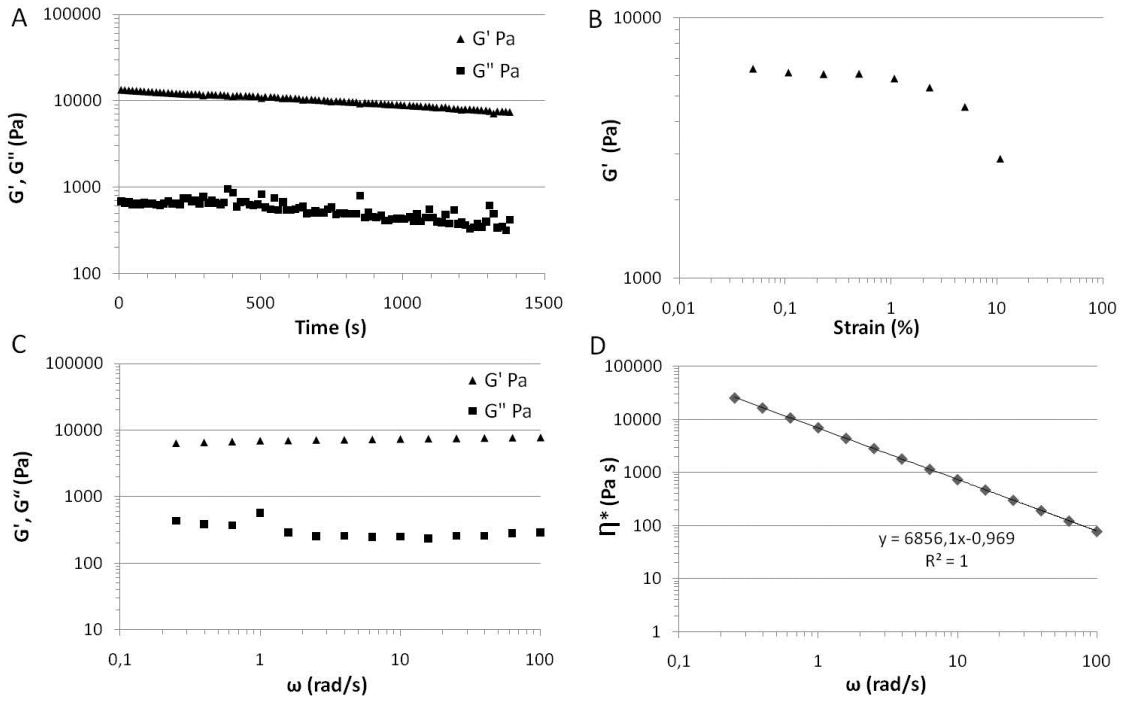

Figure 4. <u>Rheological analysis</u>. (A) G', G'' versus time; (B) G' versus strain. (C) G', G'' and (D) viscosity (η) values depending on the shear rate.

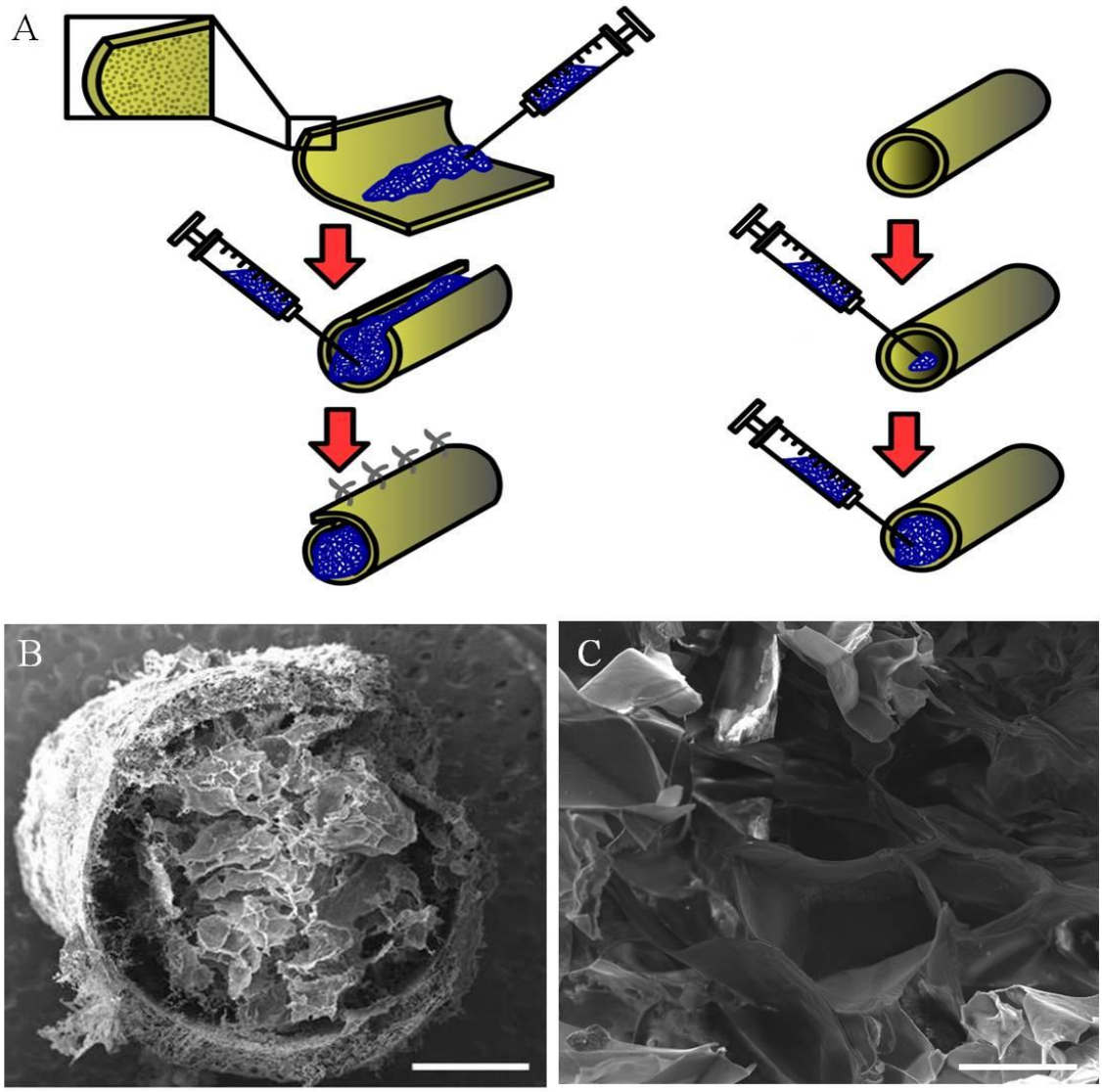

Figure 5. (A) Scheme of hydrogel injection into nerve guides (wrapped during surgery or fabricated as a tube) (B) SEM micrograph of porous PCL hollow guide filled with A/GL_GP hydrogels after freeze-drying (scale bar 500 μm) (C) SEM micrograph of freeze-dried A/GL_GP hydrogels (scale bar 200 μm).

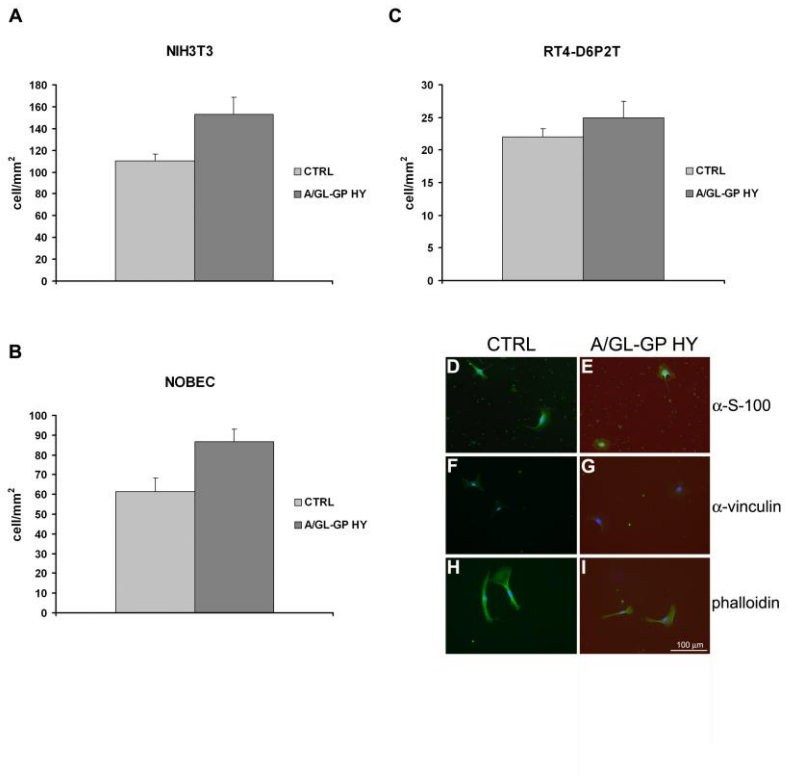

Figure 6. Cell adhesion assay. NIH3T3 (A), NOBEC (B) and RT4-D6P2T (C) cell adhesion rate measured 5 hours after seeding on polystyrene plates (CTRL) and on A/GL_GP hydrogel (A/GL-GP HY).

Representative pictures of RT4-D6P2T, cultured after anti-S-100 **(D-E)**, anti-vinculin **(F-G)** and phalloidin staining **(H-I).** There is no statistical difference between the number of adherent cells on control condition and A/GL_GP hydrogel (t-test* = $p<0.05$, ** = $p<0.01$*** = $p<0.001$) . Scale bar 100 µm.

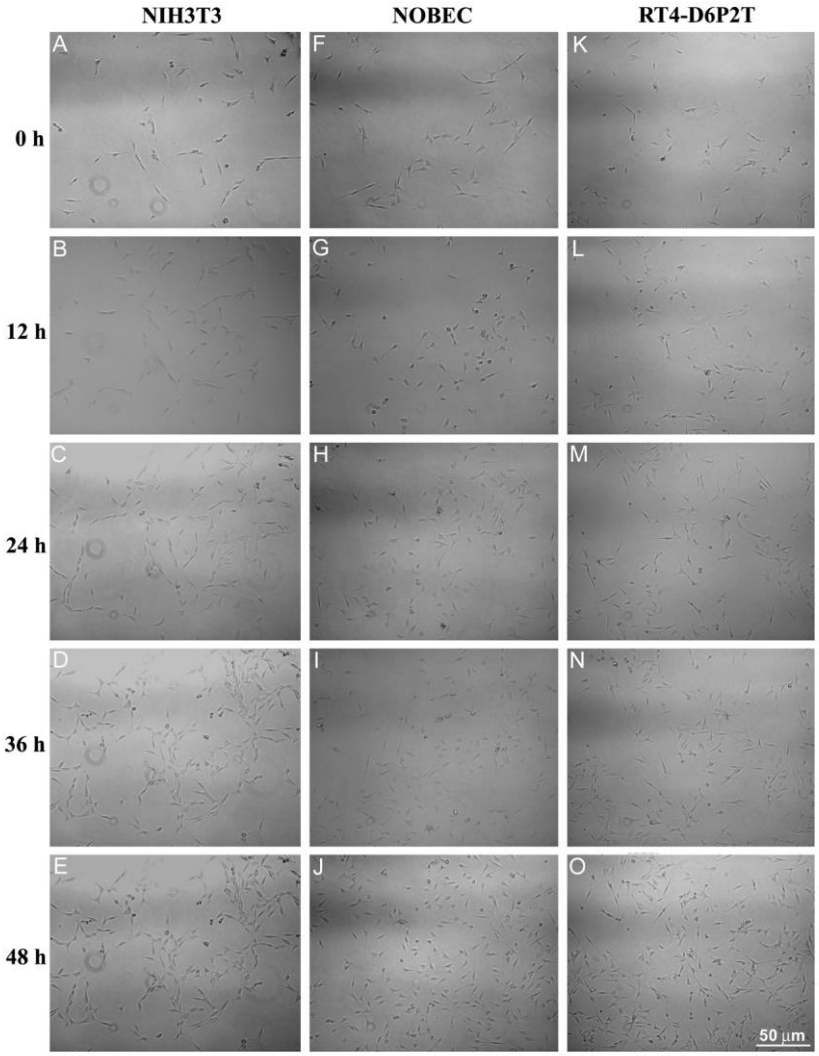

Figure 7. Time Lapse analysis. Representative pictures obtained by time lapse recording of NIH3T3 (A-E), NOBEC (F-J) and RT4-D6P2T (K-O) cells 0, 12, 24, 36 and 48 hours after plating . Scale bar 50 µm.

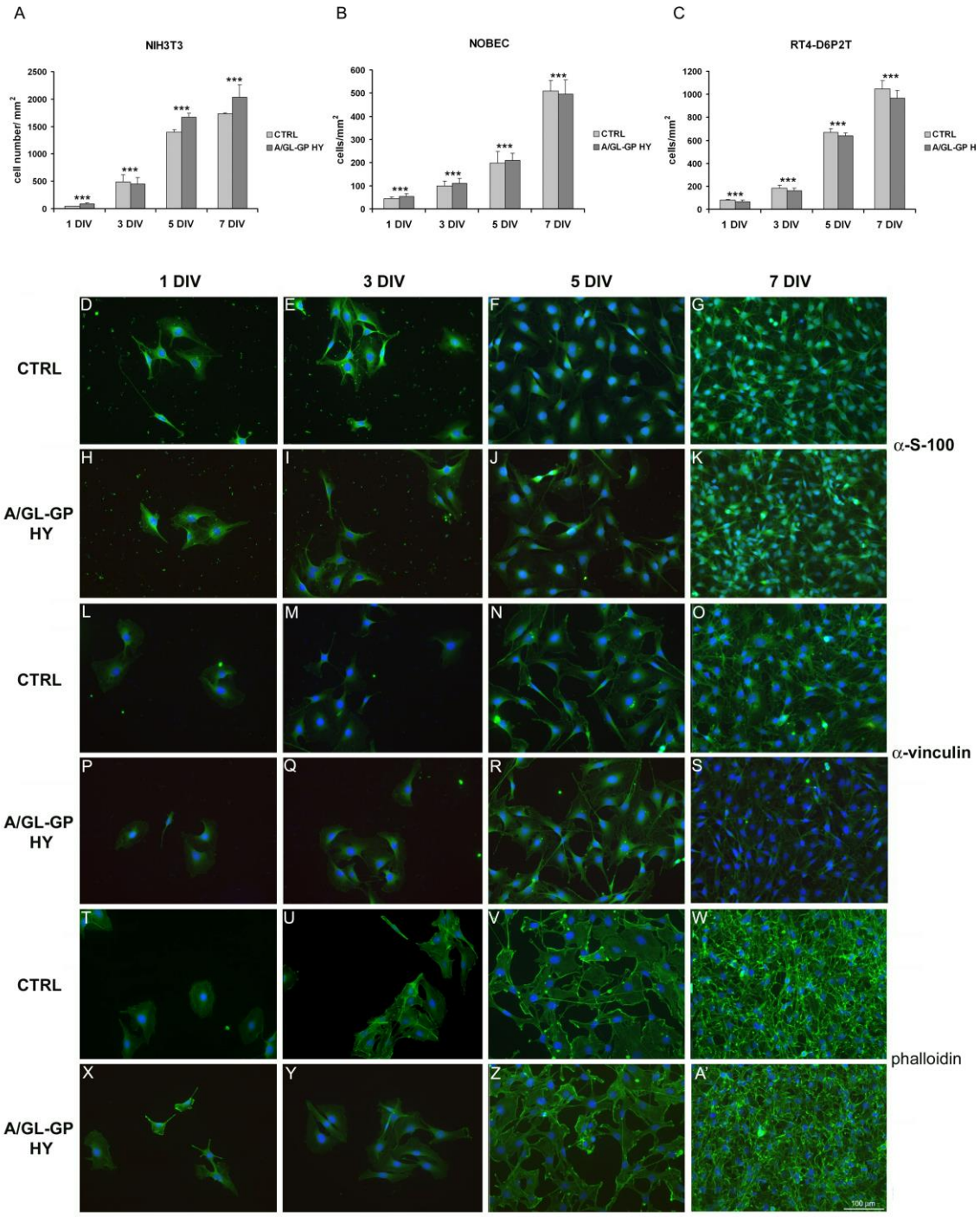

Figure 8. Cell proliferation assay. NIH3T3 **(A)**, NOBEC **(B)** and RT4-D6P2T **(C)** cell proliferation rate after 1, 3, 5 and 7 days in culture (DIV). Representative pictures of RT4-D6P2T, cultured on control condition and A/GL-GP hydrogel, after anti-S-100 **(D-K)**, anti-vinculin **(L-S)** and phalloidin staining **(T-A').** There is no significant statistical

difference between the number of proliferating cells on control condition and A/GL_GP hydrogel for each time point. There is a significant increase of cell number between time points for both control condition and A/GL_GP hydrogel (ANOVA one-way, post hoc Bonferroni, * = p≤0.05; ** = p≤0.01; *** = p≤0.001). Scale bar 100 μm.

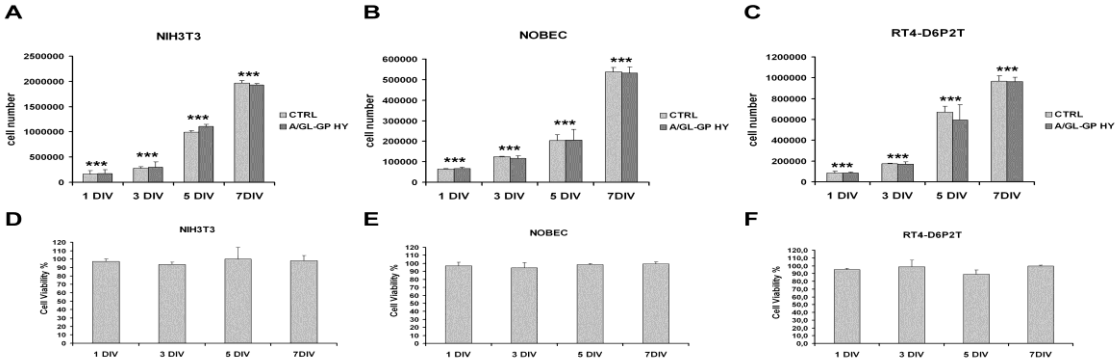

Figure 9. Cell viability and cytotoxicity assay: MTT assay. NIH3T3, NOBEC and RT4-D6P2T cell viability was analyzed by MTT assay. Number of cells **(A-C)** and cell viability percentage **(D-F)** were calculated at the different time points, on A/GL-GP hydrogel compared to control condition. There is no significant statistical difference between the number of viable cells on control condition and A/GL_GP hydrogel for each time point. There is a significant increase of cell number between time points for both control condition and A/GL_GP hydrogel (ANOVA one-way, post hoc Bonferroni, * = p≤0.05; ** = p≤0.01; *** = p≤0.001).

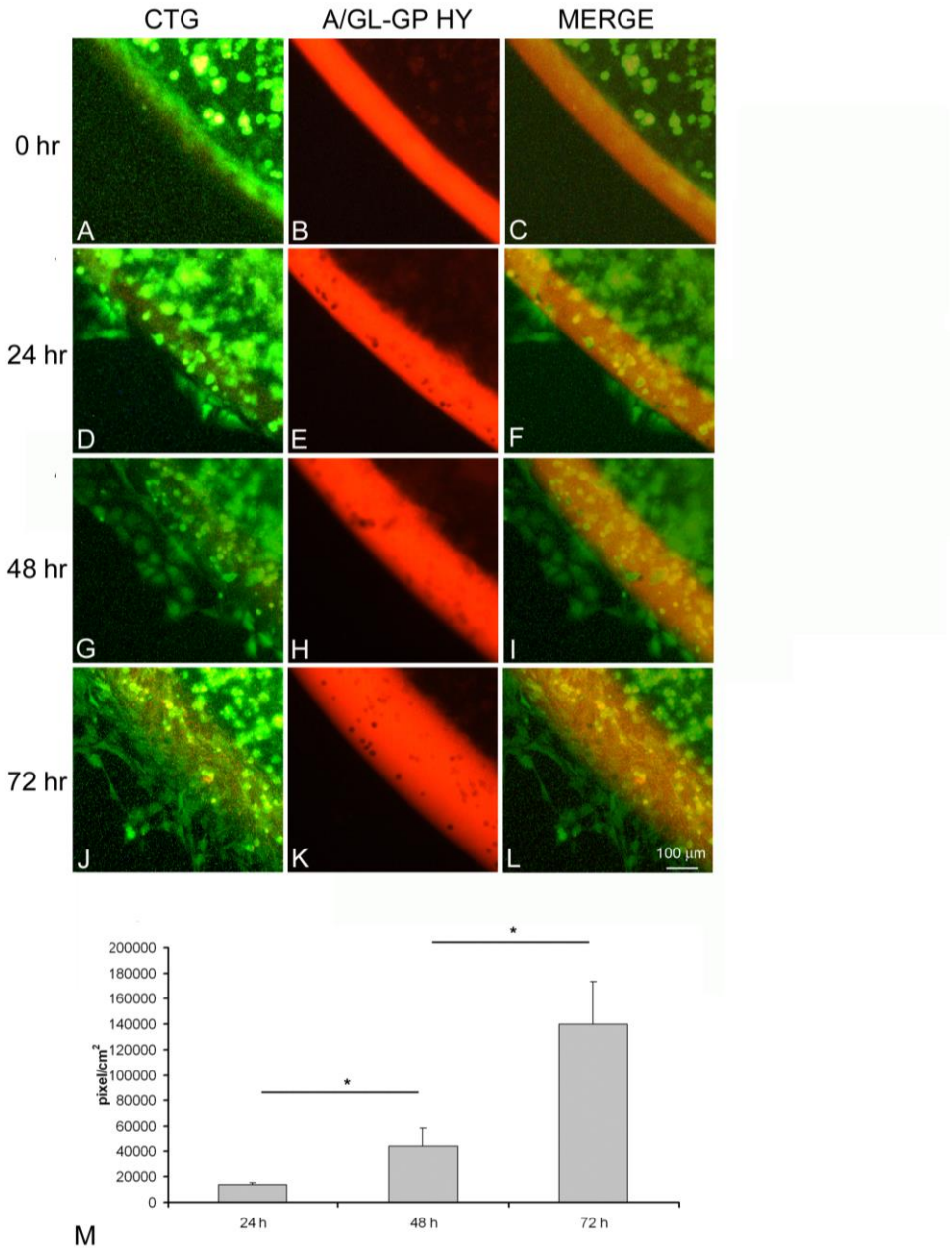

Figure 10. Three-dimensional migration assay. Representative pictures of migrated NOBEC cells 0, 24, 48 and 72 hours after incorporation in A/GL-GP hydrogel. Cells were stained with cell tracker green (CTG) and visualized in green (A, D, G and J). Biomaterial antoflurescence is visualized in red (B, E, H and K). Merge (C, F, I and L).The area occupied by cells migrated out of the drop calculated after 24, 48, 72 hours is reported (M). There is a significant increase of area occupied by migrating cells

between time points (ANOVA one-way, post hoc Bonferroni, * * = $p \leq 0.05$; ** = $p \leq 0.01$; *** = $p \leq 0.001$). Scale bar 100 μm.

References

Alzari V, Nuvoli D, Scognamillo S, Piccinini M, Gioffredi E, Malucelli G, Marceddu S, Sechi M, Sanna V, Mariani A. 2011, Graphene-containing nanocomposite hydrogels of poly(Nisopropylacrylamide) prepared by frontal polymerization, *J Mater Chem*, **21(24)**: 8727-8733

Balgude AP,Yu X, Szymanski A, Bellamkonda RV. 2001, Agar gel sti!ness determines rate of DRG neurite extension in 3D cultures, *Biomaterials*, **2**: 1077-1084

Chiono V, Pulieri E, Vozzi G, Ciardelli G, Ahluwalia A, Giusti P. 2008, Genipin-crosslinked chitosan/gelatin blends for biomedical applications, *J Mater Sci Mater Med*, **19(2)**: 889-898

Chiono V, Tonda-Turo C, Ciardelli G. 2009, Artificial scaffolds for peripheral nerve reconstruction, *Int Rev Neurobiol*, **87**: 173-199

Cordeiro PG, Seckel BR, Lipton SA, D'Amore PA, Wagner J, Madison R. 1989, Acidic fibroblast growth factor enhances peripheral nerve regeneration in vivo, *Plast Reconstr Surg*, **83**: 1013–1019

Crompton KE, Goud JD, Bellamkonda RV, Gengenbach TR, Finkelstein DI, Horne MK, Forsythe JS. 2007, Polylysine-functionalised thermoresponsive chitosan hydrogel for neural tissue engineering, *Biomaterials*, **28**: 441–449

Deligkaris K, Tadele ST, Olthuis W, van den Berg A. 2010, Hydrogel-based devices for biomedical applications, *Sensors Actuat B*, **147**: 765–774

Freile-Pelegrın Y, Murano E. 2005, Agars from three species of Gracilaria (Rhodophyta) from Yucatan Peninsula, *Bioresour Technol*, **96**: 295-302

Goodman MN, Silver J, Jacobberger JW. 1993, Establishment and neurite outgrowth properties of neonatal and adult rat olfactory bulb glial cell lines, *Brain Res*, **619**: 199-213

Guérout N, Paviot A, Bon-Mardion N, Duclos C, Genty D. 2011, Co-Transplantation of Olfactory Ensheathing Cells from Mucosa and Bulb Origin Enhances Functional Recovery after Peripheral Nerve Lesion, *PLoS ONE*, **6(8)**: e22816

Guvendiren M, Lu HD, Burdick JA. 2012, Shear-thinning hydrogels for biomedical applications, *Soft Matter*, **8**: 260-272

Lyons JG, Geever LM, Nugent MJD, Kennedy JE, Higginbotham CL. 2009, Development and characterisation of an agar – polyvinyl alcohol blend hydrogel, *J Mech Behav Biomed*, **2**: 485-493

Macosko C. 1994, *Rheology: Principles, Measurements and Application*, Wiley/VCH, Poughkeepsie, NY ISBN: 0-471-18575-2

Madison R, Da Silva CF, Dikkes P, Chiu TH, Sidman RL. 1985, Increased rate of peripheral nerve regeneration using bioresorbable nerve guides and a laminin-containing gel, *Exp Neurol*, **88**: 767–772

Mahoney MJ, Anseth KS. 2006, Three-dimensional growth and function of neural tissue in degradable polyethylene glycol hydrogels, *Biomaterials*, **27**: 2265–2274

Marten PJ, Bryant SJ, Anseth KS. 2003, Tailoring the Degradation of Hydrogels Formed from Multivinyl Poly(ethylene glycol) and Poly(vinyl alcohol) Macromers for Cartilage Tissue Engineering, *Biomacromol,* **4(2)**: 283-292

Meena R, Prasad K, Siddhanta AK. 2007, Preparation of Genipin-Fixed Agar Hydrogel, *J Appl Pol Sci*, **104**: 290–296

Muyonga JH, Cole CGB., Duodu KG. 2004, Fourier transform infrared (FTIR) spectroscopic study of acid soluble collagen and gelatin from skins and bones of young and adult Nile perch (*Lates niloticus)*, *Food Chem*, **86**: 325–332

Parrinello S, Napoli I, Ribeiro S, Digby PW, Fedorova M, Parkinson DB, Doddrell RDS., Nakayama M, Adams RH, Lloyd AC. 2010, EphB Signaling Directs Peripheral Nerve Regeneration through Sox2-Dependent Schwann Cell Sorting, *Cell*, **143**: 145-155

Praiboon J, Chirapart A, Akakabe Y, Bhumibhamon O, Kajiwara T. 2006, Physical and Chemical Characterization of Agar Polysaccharides Extracted from the Thai and Japanese Species of Gracilaria, *ScienceAsia,* **32(1)**: 11-17

Quaglia F, 2008, Bioinspired tissue engineering: the great promise of protein delivery technologies. *Int J Pharm*, **364(2)**: 281-297

Radtke C, Kocsis JD, Vogt PM. 2009, Transplantation of olfactory ensheathing cells for peripheral nerve regeneration, *Int Rev Neurobiol*, **87**:405-15

Sakiyama SE, Schense JC, Hubbell JA. 1999, Incorporation of heparin-binding peptides into fibrin gels enhances neurite extension: an example of designer matrices in tissue engineering, *FASEB J*, **13**: 2214 – 2224

Seckel BR, Jones D, Hekimian KJ, Wang KK, Chakalis DP, Costas PD. 1995, Hyaluronic acid through a new injectable nerve guide delivery system enhances peripheral nerve regeneration in the rat, *J Neurosci Res*, **40**: 318–324

Slaughter BV, Khurshid SS, Fisher OZ, Khademhosseini A, Peppas NA. 2009, Hydrogels in regenerative medicine, *Adv Mater*, **21**: 3307–3329

Sorrell JM, Caplan AI. 2009, Fibroblasts-a diverse population at the center of it all, *Int Rev Cell Mol Biol*, **276**: 161–214

Steinert AF, Weber M, Kunz M, Palmer GD, Noth U, Evans CH, Murray MM. 2008, In situ IGF-1 gene delivery to cells emerging from the injured anterior cruciate ligament, *Biomaterials*, **29**: 904-916

Tonda-Turo C, Audisio C, Gnavi S, Chiono V, Gentile P, Raimondo S, Geuna S, Perroteau I, Ciardelli G. 2011, Porous poly(ε-caprolactone) nerve guide filled with porous gelatin matrix for nerve tissue engineering, *Adv Eng Mater*, **13(5)**: B151-B164

Tonda-Turo C, Gentile P, Saracino S, Chiono V, Nandagiri VK, Muzio G, Canuto RA, Ciardelli G. 2011, Comparative analysis of gelatin scaffolds crosslinked by genipin and silane coupling agent, *Int J Biol Macromol*, **49(4)**: 700-706

Tonda-Turo C, Cipriani E, Gnavi S, Chiono V, Mattu C, Gentile P, Perroteau I, Zanetti M Ciardelli G. 2013, Crosslinked gelatin nanofibres: preparation, characterization and in vitro studies using glial-like cells, *Mater Sci Eng C*, **33**: 2723–2735

Wells MR, Kraus K, Batter DK, Blunt DG, Weremowitz J, Lynch SE, Antoniades HN, Hansson HA. 1997, Gel Matrix Vehicles for Growth Factor Application in Nerve Gap Injuries Repaired with Tubes: A Comparison of Biomatrix, Collagen, and Methylcellulose, *Exp Neurol*, **146**: 395–402

Willert SM, Sakiyama-Elbert SE. 2007, Approaches to neural tissue engineering using scaffolds for drug delivery, *Adv Drug Deliv Rev*, **59**: 325–338

Williams LR, Danielsen N, Muller H, Varon S. 1987, Exogenous matrix precursors promote functional nerve regeneration across a 15 mm gap within a silicone chamber in the rat, *J Comp Neurol*, **264**: 284–290